Applied Surface Science 488 (2019) 434–444

Contents lists available at ScienceDirect

Applied Surface Science

journal homepage: www.elsevier.com/locate/apsusc

Full length article

C_2 oxygenates formation from syngas over the promoter M(M = Rh, Co) monolayer-modified Cu(111) surface: Probing into the role of monolayer promoter on the selectivity

Baojun Wang, Weisheng Guo, Lixia Ling, Riguang Zhang*

Key Laboratory of Coal Science and Technology of Ministry of Education and Shanxi Province, Taiyuan University of Technology, Taiyuan 030024, Shanxi, PR China

ARTICLE INFO

Keywords:
Cu-based catalyst
Monolayer promoter
CH_x formation
C_2 oxygenates
Selectivity

ABSTRACT

The promoter metal monolayer deposited over other metal substrate exhibits excellent catalytic performance, in this study, the mechanism of syngas conversion to C_2 oxygenates over the promoter M(M = Rh, Co) monolayer-modified Cu catalysts have been systematically investigated to identify the role of monolayer promoter M and its effect on the selectivity using density functional theory calculations. Here, two key steps are examined, including the formation of key CH_x intermediates and the C—C bond formation of C_2 oxygenates. The results show that compared to the pure Cu catalyst, the promoter Co monolayer-modified Cu catalyst exhibits higher selectivity towards $CH_x(x = 1–3)$ formation instead of methanol, the most favored CH_x monomer is CH_2; whereas $CH_x(x = 1,2)$ is the most favored CH_x monomer on the promoter Rh monolayer-modified Cu(111), which is competitive with methanol formation. The favored CH_x monomer originates from the C—O bond cleavage of $CH_xO(x = 1,2)$ and $CH_xOH(x = 1,2)$ species formed by CO hydrogenation. Starting from the favored CH_x monomer, compared to the pure Cu catalyst, C_2 oxygenates formed by CHO insertion into CH_x is the most favorable over the promoter Rh and Co monolayer-modified Cu catalysts. In general, the promoter Co monolayer-modified Cu catalyst exhibits higher selectivity towards syngas conversion to C_2 oxygenates than the promoter Rh monolayer-modified Cu, as well as the pure Cu, Rh and Co catalysts, the reasons is attributed to that the *d*-band center of Co monolayer-modified Cu is the closest to Fermi level leading to the enhancement of adsorption capacity of the intermediates, and promoting the C—O bond activation as well as reducing the repulsion interaction between CH_x and CHO to facilitate the formation of C_2 oxygenates. The present study provides useful information for the design of highly efficient catalysts with the metal promoter monolayer-modified metal substrate in syngas conversion to C_2 oxygenates.

1. Introduction

Syngas (CO and H_2) can be converted into different products, such as ethanol and higher alcohols [1–5]. The reaction network of C_{2+} oxygenates formation including a complicated series of reactions are constrained by kinetic and thermodynamic, which depend on the type of used catalysts [6,7]. Nowadays, the transition metal Cu- [8–10] and Rh-based [11–14] catalysts were widely applied in syngas conversion to C_2 oxygenates, in which two important steps are included: (1) H-assisted CO activation to form $CH_xO(x = 1–3)$ or $CH_xOH(x = 1,2)$, followed by its C—O bond cleavage to form CH_x intermediate; (2) the C—C bond formation by CO insertion into CH_x to CH_xCO [15–17]. Alternatively, CO insertion into CH_x to $CH_xCHO(x = 1–3)$ was easier than CO insertion into CH_x on Rh(111) and Co(0001) [18], which was also supported by the studies over the Cu(211) [19], Mn-modified Cu(211) [20] and Cu(Pd)-modified Fe(100) surfaces [21].

Nowadays, non-noble metal Cu catalysts were widely used in industry because of its high CO conversion; however, the C—O bond breakage is difficult, which leads to the low concentration of CH_x intermediate and high selectivity towards methanol [22]. To improve the selectivity of C_2 oxygenates, it is very important to inhibit CH_3OH production and/or promote the C—O bond cleavage of $CH_xO(x = 1–3)$ or $CH_xOH(x = 1,2)$ to CH_x intermediates instead of their hydrogenation to methanol. DFT studies show that methanol was the main product on the Cu(111) [22] and (211) [23] surfaces, however, once CH_x intermediate is formed, C_2 oxygenates can be formed via CO insertion into CH_x. Co catalyst was widely applied in FTS because of its strong ability towards carbon chain growth and the C—O bond breakage; the main products are higher carbon hydrocarbons [24–27]. Rh-based catalysts present better catalytic performance towards syngas conversion to

* Corresponding author.
E-mail address: zhangriguang@tyut.edu.cn (R. Zhang).

https://doi.org/10.1016/j.apsusc.2019.05.033
Received 14 January 2019; Received in revised form 12 April 2019; Accepted 4 May 2019
Available online 17 May 2019
0169-4332/ © 2019 Elsevier B.V. All rights reserved.

ethanol than other transition metals, DFT calculations [28] revealed that Fe-promoted Rh(111) exhibited high selectivity towards ethanol formation, however, Rh-based catalyst is restricted in a large-scale application due to its high cost [29].

Combined with the characteristics of the metal Cu, Co and Rh, extensive studies have focused on the RhCu and CoCu bimetallic catalysts to explore its selectivity towards the formation of C_2 oxygenates from syngas [30–40]. For the Rh-modified Cu catalyst, Krishnamurthy et al. [37] explored the role of Cu in the formation rate of $CH_x(x = 1–3)$ over RhCu catalyst, suggesting that Cu decreases the catalytic activity of methane, C_2, and C_{3+} hydrocarbons formation. Zhao et al. [39] theoretically found that the individual Rh-modified Cu(111) surface improves the selectivity of C_2 oxygenates by promoting CO reaction with CH_3 in comparison with the single Rh(111) surface. Moreover, DFT studies [19] found that the individual Rh-modified Cu(211) not only inhibits methanol formation, but also promotes CH_3 formation and decreases the barriers of $CO + CH_3 \rightarrow CH_3CO$. On the other hand, Co-modified Cu catalyst has the structures of core-shell, alloy and supported types [34,35], XRD characterization [41] shows that Co is easily enriched on CoCu surface to form $Co_{shell}Cu_{core}$ structure under the syngas atmosphere. Yang et al. [34] suggested that the structure change order of CoCu alloy were Co−Cu alloy, $Cu_{core}Co_{shell}$ and $Cu_{core}Co@Co_2C_{shell}$ during the process of syngas conversion to ethanol, the selectivity of ethanol remains about 70%. Subramanian et al. [35] suggested that the Co−Cu alloy catalyst with Cu-rich (Co: Cu = 1:24) exhibited higher productivity towards ethanol than the $Co_{core}Cu_{shell}$ (Co@Cu) catalyst. DFT studies on CuCo bimetallic catalysts [33] showed that Cu sites can provide the undissociated CO and CHO and promote CHO insertion at the bimetallic sites. For the individual Co-modified Cu(211) surface [16], Cu can provide the undissociated CO and CHO, while Co boosts the C−O bond breakage leading to CH_x formation and promotes CHO/CO insertion into CH_x to C_2 oxygenates, in which the synergetic effect of Co−Cu improves the selectivity of C_2 oxygenates.

Recently, the bimetallic catalysts with transition metal promoter monolayer supported on different metal substrate catalysts have presented the excellent catalytic performances [42,43]. Shao et al. [43] found that the Pt monolayer-shell@Pd-Cu alloy-core presented much better activity towards oxygen reduction reaction than the Pt monolayer-shell@Pd-core, which is attributed to the effects of the strain and ligand between Pt monolayer and substrate, shifting *d*-band center changes the adsorption energy and the reaction activity. DFT calculations by Li et al. [44] found that CO dissociation barrier is dramatically reduced and the barrier of $CO + CH_3 \rightarrow CH_3CO$ is only 28.9 kJ·mol^{-1} on the full Mn monolayer deposited Rh(100) compared to the single Rh (100) and half Mn monolayer-deposited Rh(100). As mentioned above, for the promoter Rh and Co-modified Cu catalysts, up to now, few studies are reported to investigate the role of monolayer promoter and its effect on the selectivity of C_2 oxygenate in syngas conversion.

Aiming at illustrating above issues, this study has systematically examined the underlying mechanism of syngas conversion to C_2 oxygenates over the promoter Rh and Co monolayer-modified Cu catalysts, including the formation of $CH_x(x = 1–3)$ together with methanol, and CO/CHO insertion into CH_x to C_2 oxygenates; Here, the density functional theory calculations are employed. Meanwhile, in comparison with the single Cu catalyst, the role of monolayer promoter Rh and Co and their effects on the selectivity of C_2 oxygenates are identified.

2. Computational details

Since (111) is mainly exposed and stable surface of Cu catalyst under syngas conversion [45], Cu(111) surface is selected to present the characteristic of Cu catalyst. Cu(111) surface is modeled using a four-layer $p(3 \times 3)$ supercell, in which the bottom one layers is fixed, whereas the upper three layers with the adsorbates are relax. The vacuum is 15 Å to avoid the interaction between the slabs. For the Rh and Co monolayer-modified Cu catalysts, the top-layer Cu atoms of Cu(111) surface are replaced by the Rh or Co atoms, respectively, as shown in Fig. 1, two surfaces are denoted as Rh_{ML}/Cu(111) and Co_{ML}/Cu(111), respectively.

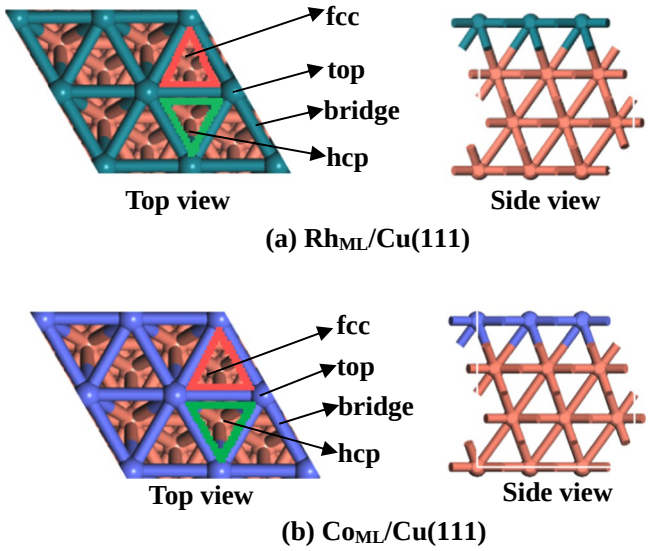

Fig. 1. The surface morphology and its adsorption sites of (a) Rh_{ML}/Cu(111) and (b) Co_{ML}/Cu(111) surfaces. Cu, Co and Rh atoms are shown in the orange, purple and dark cyan balls, respectively. (For interpretation of the references to color in this figure legend, the reader is referred to the web version of this article.)

All DFT calculations are performed using the Vienna Ab-initio Simulation Package (VASP) [46,47]. The generalized gradient approximation (GGA) with PBE [48] was used as the exchange-correlation functional. The convergence criteria for geometry optimization was set to be 5×10^{-6} eV for the energy differences and 0.01 eV·Å^{-1} for the forces. A plane-wave cutoff energy of 500 eV is employed. The surface Brillouin zone is selected as a $3 \times 3 \times 1$ *k*-point [49]. The dimer method is used to optimize the transition states [50,51]. The transition state of elementary reactions was obtained by the climbing-image nudged elastic band method (CI-NEB) [51,52]. The convergence criteria of the optimized transition state is that the forces of all atoms are less than 0.05 eV·Å^{-1}. Meanwhile, the vibrational frequency is also calculated to confirm the transition state with the single imaginary frequency.

Syngas conversion to C_{2+} oxygenates on the Cu-based, Rh-based and Co-based catalysts usually occurs at 500–600 K [7,35], in this study, the Gibbs free energy for syngas conversion to C_2 oxygenates is calculated at 500 K, which includes the contributions of entropy and thermal energy [53]. The detailed descriptions about the calculations of Gibbs free energy are presented in the Supplementary Material.

3. Results and discussion

3.1. Adsorption of reactants, intermediates and products

Figs. S1 and S2 present the most stable adsorption configurations of reactants, intermediates and products in syngas conversion to C_2 oxygenates on Rh_{ML}/Cu(111) and Co_{ML}/Cu(111) surfaces, respectively. Correspondingly, the adsorption energy, the stable adsorption site and the bond length of key intermediates are listed in Tables S1 and S2. Tables 1 and 2 list the activation and reaction free energies of each elementary reaction on the Rh_{ML}/Cu(111) and Co_{ML}/Cu(111) at 500 K, respectively.

Table 1
The activation free energy (ΔG_a/kJ·mol^{-1}) and reaction free energies (ΔG/kJ·mol^{-1}) of the elementary reactions involving in syngas conversion to C_2 oxygenates at 500 K on Rh_{ML}/Cu(111) surface.

	Elementary reactions	Transition state	ΔG_a	ΔG
R1-1	CO → C + O	TS1-1	367.1	287.6
R1-2	CO + H → CHO	TS1-2	155.3	104.4
R1-3	CO + H(1) → COH	TS1-3	154.5	64.8
R1-4	CHO + H → CH_2O	TS1-4	76.9	38.9
R1-5	CHO + H(1) → CHOH	TS1-5	75.5	4.0
R1-6	COH + H → CHOH	TS1-6	121.5	58.6
R1-7	CH_2O + H → CH_3O	TS1-7	73.3	31.5
R1-8	CH_2O + H(1) → CH_2OH	TS1-8	79.6	12.5
R1-9	CHOH + H → CH_2OH	TS1-9	69.5	22.6
R1-10	CHO → CH + O	TS1-10	191.5	58.4
R1-11	CHOH→CH + OH	TS1-11	104.8	3.3
R1-12	CH_2O → CH_2 + O	TS1-12	127.3	36.2
R1-13	CH_2OH → CH_2 + OH	TS1-13	77.7	5.6
R1-14	CH_3O → CH_3 + O	TS1-14	148.7	−38.3
R1-15	CH_3O + H → CH_3OH	TS1-15	58.4	−20.9
R1-16	CH_2OH + H → CH_3OH	TS1-16	82.6	17.7
R1-17	CH + H → CH_2	TS1-17	83.7	44.2
R1-18	CH + CO → CHCO	TS1-18	137.6	100.1
R1-19	CH + CH → C_2H_2	TS1-19	122.1	24.4
R1-20	CH + CHO → CHCHO	TS1-20	77.0	30.4
R1-21	CH_2 + H → CH_3	TS1-21	65.4	−2.0
R1-22	CH_2 + CH_2 → C_2H_4	TS1-22	104.4	−46.2
R1-23	CH_2 + CO → CH_2CO	TS1-23	134.7	75.5
R1-24	CH_2 + CHO → CH_2CHO	TS1-24	70.3	−24.7
R1-25	CH_2 → CH + H	TS1-25	39.5	−44.2

Table 2
The activation free energy barriers (ΔG_a/kJ·mol^{-1}) and reaction free energies (ΔG/kJ·mol^{-1}) of elementary reactions involving in syngas conversion to C_2 oxygenates at 500 K on Co_{ML}/Cu(111) surface.

	Elementary reactions	Transition state	ΔG_a	ΔG
R2-1	CO → C + O	TS2-1	298.2	10.0
R2-2	CO + H → CHO	TS2-2	142.1	121.7
R2-3	CO + H → COH	TS2-3	167.4	92.3
R2-4	CHO + H → CH_2O	TS2-4	61.9	60.7
R2-5	CHO + H(1) → CHOH	TS2-5	118.5	84.8
R2-6	COH + H → CHOH	TS2-6	133.6	123.1
R2-7	CH_2O + H → CH_3O	TS2-7	63.4	−36.8
R2-8	CH_2O + H(1) → CH_2OH	TS2-8	106.1	54.9
R2-9	CHO → CH + O	TS2-9	119.2	−126.4
R2-10	CHOH + H → CH_2OH	TS2-10	60.7	25.0
R2-11	CHOH→CH + OH	TS2-11	32.6	−142.0
R2-12	CH_2O → CH_2 + O	TS2-12	30.1	−119.8
R2-13	CH_2OH → CH_2 + OH	TS2-13	49.1	−102.6
R2-14	CH_3O → CH_3 + O	TS2-14	117.1	−47.8
R2-15	CH_3O + H → CH_3OH	TS2-15	149.6	104.9
R2-16	CH_2OH + H → CH_3OH	TS2-16	90.0	30.0
R2-17	CH_2 + H → CH_3	TS2-17	55.1	18.4
R2-18	CH_2 + CH_2 → C_2H_4	TS2-18	59.1	−2.0
R2-19	CH_2 + CO → CH_2CO	TS2-19	112.2	109.7
R2-20	CH_2 + CHO → CH_2CHO	TS2-20	41.5	−22.4

3.2. CO initial activation

Previous studies over the Cu(211) [19,23], (110) [54], (100) [55] and (111) [22] surfaces showed that CO initial activation was the key step in syngas conversion to C_2 oxygenates, including CO → C + O and CO + H → CHO/COH.

As presented in Fig. 2, on Rh_{ML}/Cu(111), CO direct dissociation via TS1-1 has an activation free energy of 367.1 kJ·mol^{-1}; the activation free energies of CO + H → CHO and CO + H → COH are 155.3 and 154.5 kJ·mol^{-1}, respectively. Compared to Rh(111) surface that CO initial activation to form CHO [28], the substrate Cu of Rh_{ML}/Cu(111) changes the route of CO initial activation. On Co_{ML}/Cu(111), CO direct dissociation via TS2-1 has an activation free energy of 298.2 kJ·mol^{-1}; CO hydrogenation to CHO and COH have the activation free energies of 142.1 and 167.4 kJ·mol^{-1}; similar results on the Co(111) [26] and Cu-modified Co(0001) [33] surfaces are also CO initial activation to form CHO.

As mentioned above, CO direct dissociation is hard to occur over both surfaces due to the higher dissociation barrier. On Rh_{ML}/Cu(111), CO + H → CHO and CO + H → COH are easier, whereas CO + H → CHO is the most favorable on Co_{ML}/Cu(111). On the Cu(111) [22] and (211) [23] surfaces, CO initial activation is to form CHO. These results show that the promoter Rh or Co affect the favorable route of CO initial activation.

3.3. The key intermediate CH, CH_2, CH_3 and methanol formation

Since the reaction of CO → C + O is difficult to occur on Rh_{ML}/Cu(111) and Co_{ML}/Cu(111) surfaces, all CH_x monomers should originate from the dissociation of CH_xOH(x = 1,2) and CH_xO(x = 1–3). Based on CO initial activation, for the formation of key intermediates CH, CH_2, CH_3 and CH_3OH, both CHO and COH species are used as the initial state on Rh_{ML}/Cu(111); CHO species is selected as the initial state on Co_{ML}/Cu(111).

3.3.1. CH formation

Three routes can generate CH intermediate: one is CHO → CH + O; the second is CHO + H → CHOH→CH + OH; the third is COH + H → CHOH→CH + OH.

On Rh_{ML}/Cu(111), CHO + H → CHOH is much easier in kinetics than COH + H → CHOH (75.5 vs. 121.5 kJ·mol^{-1}), as a result, only CHOH (via CHO hydrogenation) and CHO dissociation contribute to CH formation, as illustrated in Fig. 3(a), these two routes have the overall activation free energies of 213.2 and 295.9 kJ·mol^{-1}, respectively. Thus, CH is dominantly formed via CHOH dissociation.

On Co_{ML}/Cu(111), CO initial activation prefers to form CHO, thus, CH is formed via the dissociation of CHO and CHOH, as presented in Fig. 3(b), both routes are parallel and competitive for CH formation with the overall activation free energies of 240.9 and 240.2 kJ·mol^{-1}, respectively. Moreover, compared to the single Co(111) surface that CH formation via CHO direct dissociation [26], the substrate Cu of Co_{ML}/Cu(111) changes the route of CH formation.

3.3.2. CH_2 formation

CH_2 is formed via the dissociation of CH_2O or CH_2OH. As listed in Table 1, on Rh_{ML}/Cu(111), CHO + H → CH_2O is competitive with CHO + H → CHOH in kinetics (76.9 vs. 75.5 kJ·mol^{-1}), however, CHOH + H → CH_2OH is easier than CH_2O + H → CH_2OH (69.5 vs. 79.6 kJ·mol^{-1}), namely, CH_2OH prefers to be formed by CHOH hydrogenation. Thus, as presented in Fig. 4(a), CH_2 formation has two routes of CH_2O → CH_2 + O and CHOH + H → CH_2OH → CH_2 + OH with the overall activation free energies of 270.6 and 208.7 kJ·mol^{-1}, respectively, the latter route mainly contribute to CH_2 formation via CH_2OH dissociation.

On Co_{ML}/Cu(111), CHO + H → CHOH is unfavorable in kinetics compared to CHO + H → CH_2O (118.5 vs. 61.9 kJ·mol^{-1}), CH_2OH dominantly come from CH_2O hydrogenation. Thus, CH_2 formation has two routes, see Fig. 4(b), CH_2O → CH_2 + O and CH_2O + H → CH_2OH → CH_2 + OH, the former is more favorable than the latter in kinetics (212.5 vs. 288.5 kJ·mol^{-1}). Further, compared to Co(111) (65.3 kJ·mol^{-1}) [26], Co_{ML}/Cu(111) is more beneficial for CH_2O direct dissociation (30.1 kJ·mol^{-1}).

3.3.3. CH_3 and methanol formation

CH_3 formation has only one route via CH_3O → CH_3 + O. Meanwhile, CH_3O or CH_2OH hydrogenation can also form methanol, which affects the production of CH_x intermediates and C_2 oxygenates.

On Rh_{ML}/Cu(111) (Fig. 5(a)), the overall barrier of CH_3 formation is 323.5 kJ·mol^{-1}. Meanwhile, CH_2OH is mainly formed by CHOH

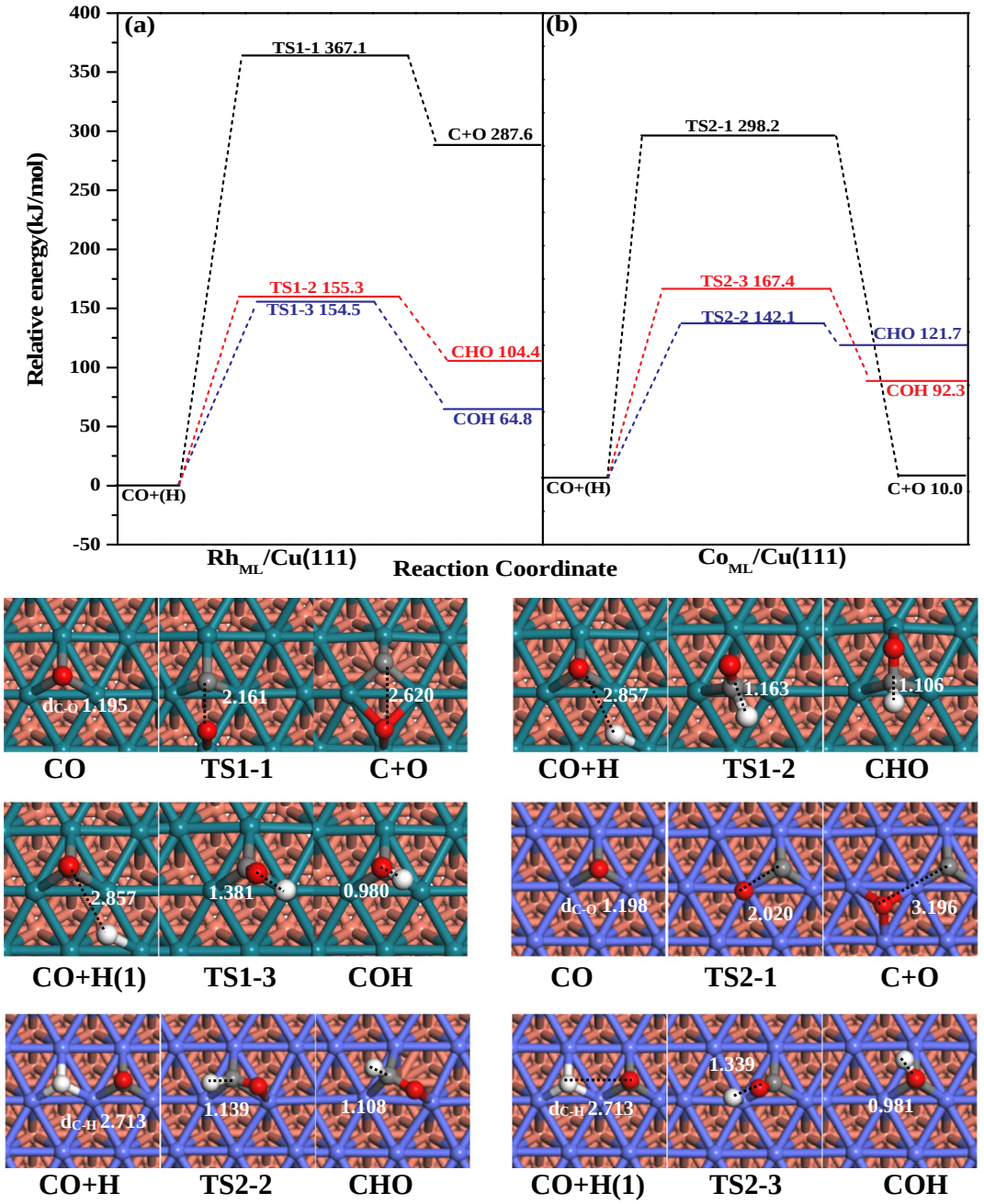

Fig. 2. The potential energy profile for CO initial activation on $Rh_{ML}/Cu(111)$ and $Co_{ML}/Cu(111)$ surfaces together with initial state, transition state and final state. Bond lengths are in Å. Gray, red, and white balls denote C, O and H atoms, respectively. (For interpretation of the references to color in this figure legend, the reader is referred to the web version of this article.)

hydrogenation, namely, methanol formation may undergoes the routes via CHOH, CH_2OH species and that via CH_2O, CH_3O species, respectively, the former route is more favorable than the latter in kinetics (213.6 vs. 233.2 kJ·mol^{-1}). Thus, the production of methanol is much higher than CH_3 in kinetics (213.6 vs. 323.5 kJ·mol^{-1}) on $Rh_{ML}/Cu(111)$, whereas $CH_3O \rightarrow CH_3 + O$ is competitive with $CH_3O + H \rightarrow CH_3OH$ on Rh(111) [28], suggesting that $Rh_{ML}/Cu(111)$ promotes methanol formation.

On $Co_{ML}/Cu(111)$ (see Fig. 5(b)), CH_3 formation has an overall barrier of 262.7 kJ·mol^{-1}. Two routes of methanol formation are $CH_3O + H \rightarrow CH_3OH$ and $CH_2OH + H \rightarrow CH_3OH$ with the overall barriers of 295.2 and 327.3 kJ·mol^{-1}, respectively. Thus, CH_3 formation is more favorable than methanol on $Co_{ML}/Cu(111)$ (262.7 vs. 295.2 kJ·mol^{-1}). In contrast, on Co(111) [26], $CH_3O \rightarrow CH_3 + O$ competes with $CH_3O + H \rightarrow CH_3OH$ (142.9 vs. 148.6 kJ·mol^{-1}), namely, $Co_{ML}/Cu(111)$ effectively inhibit methanol formation.

3.4. The effect of Rh and Co on the favored CH_x monomer and methanol

As mentioned above, on $Rh_{ML}/Cu(111)$, the preferential formation route of $CH_x(x = 1–3)$ and methanol correspond to the dissociation of CHOH, CH_2OH and CH_3O, as well as CH_3O hydrogenation, which have the overall barriers of 213.2, 208.7, 323.5 and 213.6 kJ·mol^{-1}, respectively. Thus, the favored CH_x monomer is $CH_x(x = 1,2)$, which competes with methanol formation.

On $Co_{ML}/Cu(111)$, $CH_x(x = 1–3)$ and methanol formation corresponds to the favored routes via CHO, CHOH, CH_2O and CH_3O dissociation, as well as CH_3O hydrogenation with the overall barriers of

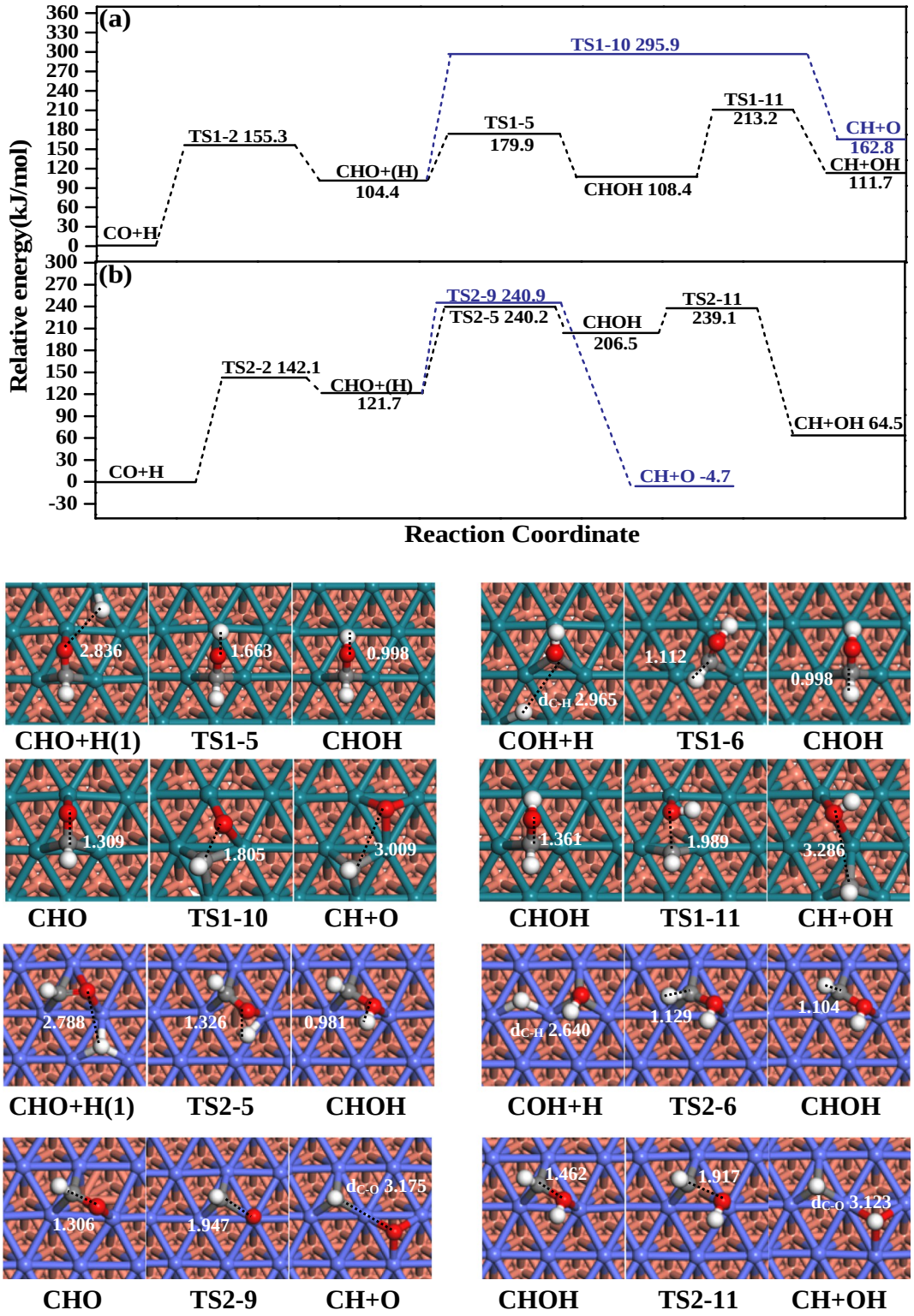

Fig. 3. The potential energy profile for CH formation on Rh_{ML}/Cu(111) and Co_{ML}/Cu(111) surfaces together with initial state, transition state and final state. Bond lengths are in Å. See Fig. 2 for color coding.

240.9, 240.2, 212.5, 262.7 and 295.2 kJ·mol^{-1}, respectively. Thus, the favored CH_x monomer is CH_2, which is superior to methanol formation in kinetics.

On Cu(111) [22], CH_x(x = 2,3) species was the favored monomer formed by the dissociation of CH_2OH and CH_3O; methanol formation by CH_3O hydrogenation was much easier than CH_x(x = 2,3) formation. On Rh(111) [28], CH_3 was the favored CH_x monomer formed by CH_3O dissociation; methanol formation by CH_3O hydrogenation is also easier than CH_3 formation. Whereas CH is the favored CH_x monomer, which is much easier than methanol on Co(111) [26].

Compared to Rh(111), Co(111) and Cu(111) surfaces, aiming at a better understanding about the role of monolayer promoter Rh and Co in Rh_{ML}/Cu(111) and Co_{ML}/Cu(111), the barrier difference between the favored CH_x monomer and methanol is used as a simple descriptor to

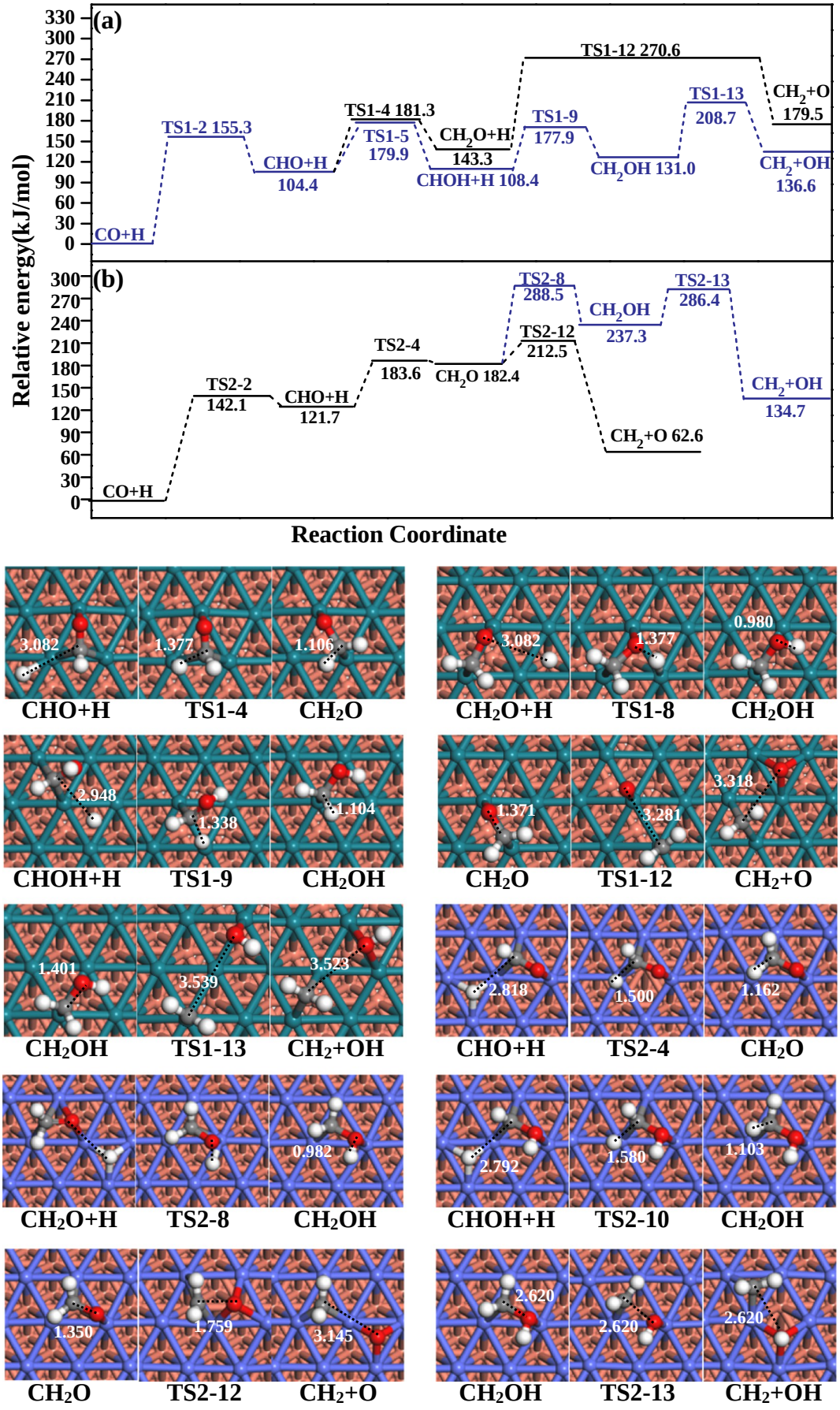

Fig. 4. The potential energy profile for CH_2 formation on Rh_{ML}/Cu(111) and Co_{ML}/Cu(111) surfaces together with initial state, transition state and final state. Bond lengths are in Å. See Fig. 2 for color coding.

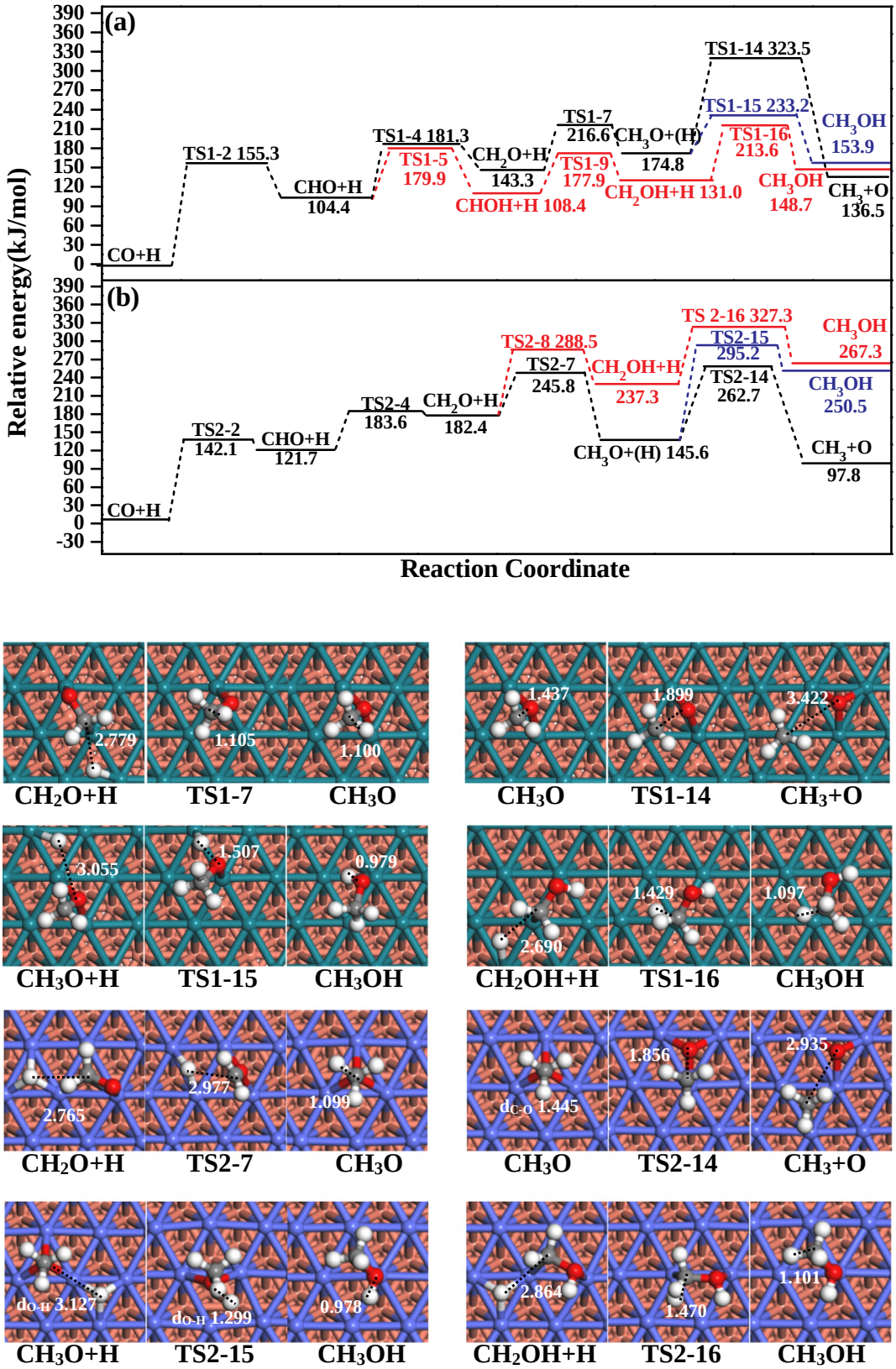

Fig. 5. The potential energy profile for CH_3 and CH_3OH formation on Rh_{ML}/Cu(111) and Co_{ML}/Cu(111) surfaces together with initial state, transition state and final state. Bond lengths are in Å. See Fig. 2 for color coding.

evaluate the selectivity of the favored CH_x monomer. Namely, the more negative barrier difference signifies the preferential formation of CH_x monomer and the lower methanol selectivity.

With respect to CO + H, as shown in Fig. 6, the overall barrier differences between methanol and the favored CH_x monomer are 13.6, 28.0, −51.1, −4.9 and −82.7 kJ·mol^{-1} over the Cu(111) [22], Rh

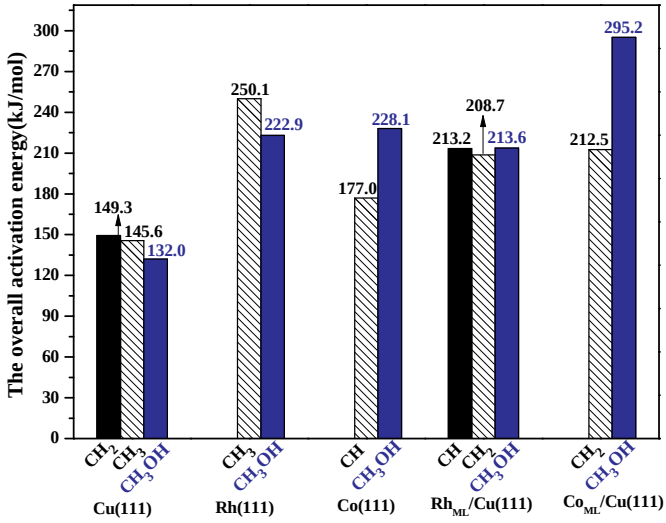

Fig. 6. The overall energy barrier of stable CH_x and CH_3OH formation on Cu (111), Rh(111), Co(111), Rh_{ML}/Cu(111) and Co_{ML}/Cu(111) surfaces, respectively.

(111) [28], Co(111) [26], Rh_{ML}/Cu(111) and Co_{ML}/Cu(111) surfaces, respectively. Among them, both Co(111) and Co_{ML}/Cu(111) significantly promote the formation of favored CH_x monomer, especially, Co_{ML}/Cu(111) is more favorable than Co(111). Secondly, Rh_{ML}/Cu (111) slightly improve CH_x selectivity compared to Cu(111) and Rh (111). Thus, the promoter Co monolayer-modified Cu catalysts substantially promote the C—O bond breakage of $CH_xOH(x = 1,2)$ and $CH_xO(x = 1–3)$ species to form CH_x intermediate and inhibit CH_3OH formation, which provides enough CH_x source to react with CO/CHO leading to C_2 oxygenates.

3.5. The formation of C_2 oxygenates

Previous studies [19–21] showed that CO/CHO insertion into CH_x to CH_xCO/CH_xCHO contributed to the formation of C_2 oxygenates; meanwhile, CH_x hydrogenation and its self-coupling to C_2 hydrocarbons also occur.

As described above, the favored CH_x monomers are CH and CH_2 species on Rh_{ML}/Cu(111), and that is CH_2 on Co_{ML}/Cu(111). The reactions related to CH and CH_2 species on Rh_{ML}/Cu(111) (see Fig. 7(a)) show that $CH + H \rightarrow CH_2$ and $CHO + CH \rightarrow CHCHO$ are the first two favorable reactions; however, $CH_2 \rightarrow CH + H$ is the most favorable among all reactions related to CH_2 species. Hence, CH is the dominant CH_x monomer, and C_2 oxygenates CHCHO is the most favored product on Rh_{ML}/Cu(111). On Co_{ML}/Cu(111) (see Fig. 7(b)), $CHO + CH_2 \rightarrow CH_2CHO$ is the most favorable among all reactions related to CH_2 species. DFT studies by Ren et al. [32] on the Co-rich CuCo(111)/(211) or Cu-rich CuCo(111)/(211) surfaces also found that C_2 oxygenates prefers to be formed by CHO insertion. However, on the single Cu(111) surface [56], the favored CH_x monomer are CH_2 and CH_3, accordingly, CH_2 self-coupling to C_2H_4 and CH_3 hydrogenation to CH_4 are preferential, respectively.

As mentioned above, compared to the single Cu(111) [56], both Rh_{ML}/Cu(111) and Co_{ML}/Cu(111) can inhibit the production of methane and C_2 hydrocarbons, as a result, both Rh_{ML}/Cu(111) and Co_{ML}/Cu(111) make the product distribution more concentrated on C_2 oxygenates. Moreover, C_2 oxygenates formed by CHO insertion into $CH_x(x = 1–3)$ is more favorable in kinetics than that by CO insertion into $CH_x(x = 1–3)$, CO insertion into CH_x is strongly endothermic, whereas CHO insertion are exothermic or slightly endothermic, which is consistent with the earlier studies on Rh(111) and Co(0001) surfaces [18]. Similar results were also confirmed on the Cu(211) [19] and MnCu(211) [20] surfaces, the reasons may be that the CHO gap between HOMO and LUMO is smaller than CO, which enhanced the interaction between CHO and the catalyst [18]. In general, once the favored CH_x monomer formation, the single Cu(111) surface [56] exhibits better selectivity towards the hydrocarbons. However, both Rh_{ML}/Cu (111) and Co_{ML}/Cu(111) exhibit better selectivity towards the C_2 oxygenates CHCHO and CH_2CHO, respectively. Namely, the promoter Rh and Co monolayer-modified Cu(111) improve the selectivity of C_2 oxygenates compared to the single Cu(111), especially, the monolayer promoter Co presents better activity towards C_2 oxygenates than the monolayer promoter Rh.

3.6. The role of Rh and Co in Rh_{ML}/Cu(111), Co_{ML}/Cu(111)

It is generally known that Cu catalyst is favorable for methanol formation from syngas [9,22,23]; as a result, there are not enough CH_x sources to participate into CO/CHO insertion to form C_2 oxygenates. Since CO direct dissociation is difficult to occur over the Rh_{ML}/Cu(111), Co_{ML}/Cu(111) and Cu(111) surfaces, all $CH_x(x = 1–3)$ species should come from the C—O bond cleavage of $CH_xO(x = 1–3)$ or CH_xOH $(x = 1,2)$. By comparison, the adsorption of CH_x, O, OH, CH_xO $(x = 1–3)$ and $CH_xOH(x = 1,2)$ on Co_{ML}/Cu(111) is much stronger than those over the Rh_{ML}/Cu(111) and Cu(111) (see Table 3). On Co_{ML}/Cu (111), the favored CH_2 monomer is formed via CH_2O dissociation, the strong adsorption of CH_2O will make its C—O bond cleavage more easier to produce CH_2. Moreover, since the binding of CH_x, O and OH species on Co_{ML}/Cu(111) is stronger compared to Rh_{ML}/Cu(111) and Cu(111), a stronger thermodynamic driving force promotes the C—O bond cleavage of CH_xO and CH_xOH leading to the easier formation of CH_x intermediate over Co_{ML}/Cu(111); this agrees with our calculated kinetics results. For C_2 oxygenates formation on Rh_{ML}/Cu(111) and Co_{ML}/Cu(111), $CHO + CH_x \rightarrow CH_xCHO(x = 1–3)$ is the most favorable compared to other reactions related to $CH_x(x = 1–3)$ species.

Hence, the role of Rh and Co monolayer-modified Cu(111) surfaces can be summarized as follows in comparison with the single Cu(111) surface: (1) For $CH_x(x = 1–3)$ formation, both Rh_{ML}/Cu(111) and Co_{ML}/Cu(111) promote the C—O bond breakage of $CH_xO(x = 1–3)$ or $CH_xOH(x = 1,2)$, especially, Co_{ML}/Cu(111) substantially promote $CH_x(x = 1–3)$ formation and inhibit methanol formation. (2) For C_2 oxygenates formation, both Rh_{ML}/Cu(111) and Co_{ML}/Cu(111) promote CHO insertion into the favored $CH_x(x = 1,2)$ monomer to C_2 oxygenates; especially, Co_{ML}/Cu(111) exhibits better selectivity and activity towards C_2 oxygenates.

To investigate electronic properties of Cu(111), Rh_{ML}/Cu(111) and Co_{ML}/Cu(111) surfaces, the analysis for *p*DOS and *d*-band center is applied to provide a microcosmic interpretation. It is well-known that the *d* electrons or empty *d* orbitals of transition metal affect the catalytic activity and adsorption ability of adsorbed species. The shorter the distance between Fermi level and *d*-band center is, the better the catalytic activity is [21], and the higher the adsorption ability is [43]. The *d*-band center is obtained using the following Eq. (1) [57]:

$$\varepsilon_d = \frac{\int_{-\infty}^{+\infty} E\rho_d(E)\mathrm{d}E}{\int_{-\infty}^{+\infty} \rho_d(E)\mathrm{d}E} \quad (1)$$

The average *d*-band centers of surface metals are located at −2.42, −1.01 and −2.35 eV (see Fig. 8) corresponding to Rh_{ML}/Cu(111), Co_{ML}/Cu(111) and Cu(111) surfaces, respectively. The *d*-band center of Co_{ML}/Cu(111) is the lowest, and the corresponding $CH_xO(x = 1–3)$ and $CH_xOH(x = 1,2)$ species have the largest adsorption energy compared to Rh_{ML}/Cu(111) and Cu(111), namely, Co_{ML}/Cu(111) presents stronger activity towards the C—O bond breaking of $CH_xO(x = 1–3)$ and $CH_xOH(x = 1,2)$ species to form CH_x. These results are consistent with above kinetic results.

For C_2 oxygenate formation by $CHO + CH_x \rightarrow CH_xCHO(x = 1,2)$, both Co_{ML}/Cu(111) and Rh_{ML}/Cu(111) surfaces exhibit higher

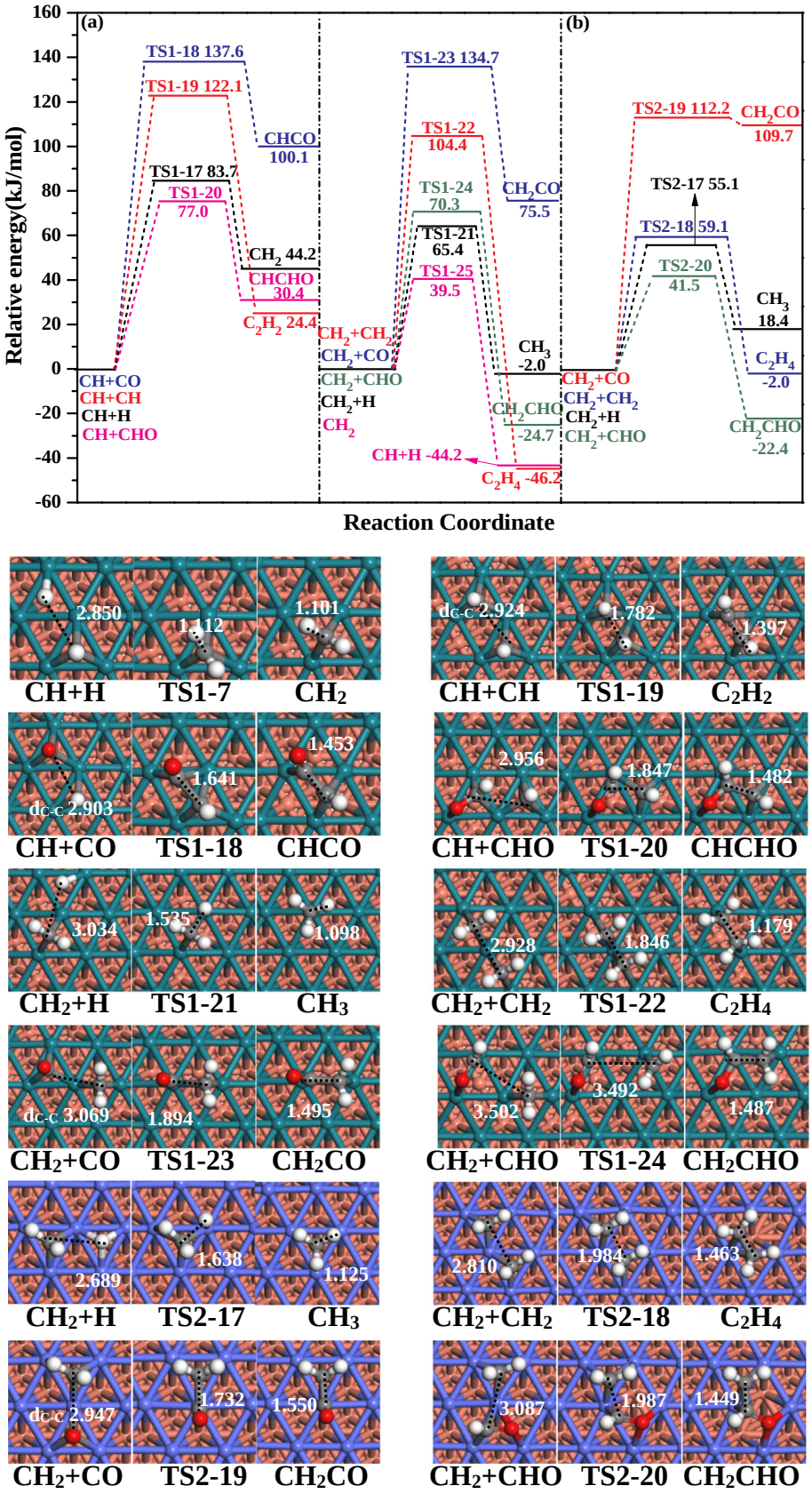

Fig. 7. The potential energy profile for reactions related to CH_x(x = 1–2) and reactions related to CH_2 on Rh_{ML}/Cu(111) and Co_{ML}/Cu(111) surfaces together with initial state, transition state and final state. Bond lengths are in Å. See Fig. 2 for color coding.

Table 3
Adsorption energy (E_{ads}/kJ·mol^{-1}) of key intermediates on Cu(111), Rh_{ML}/Cu(111) and Co_{ML}/Cu(111) surfaces.

Species	Cu(111)	Rh_{ML}/Cu(111)	Co_{ML}/Cu(111)
CH	468.2	657.6	658.9
CH_2	274.8	397.5	415.4
CH_3	111.0	189.4	200.1
O	452.5	504.4	619.5
OH	272.9	255.6	365.2
CHO	109.3	241.2	246.8
CHOH	254.2	414.2	374.5
CH_2O	33.9	80.1	87.4
CH_2OH	161.8	175.9	175.6
CH_3O	206.4	191.6	298.9

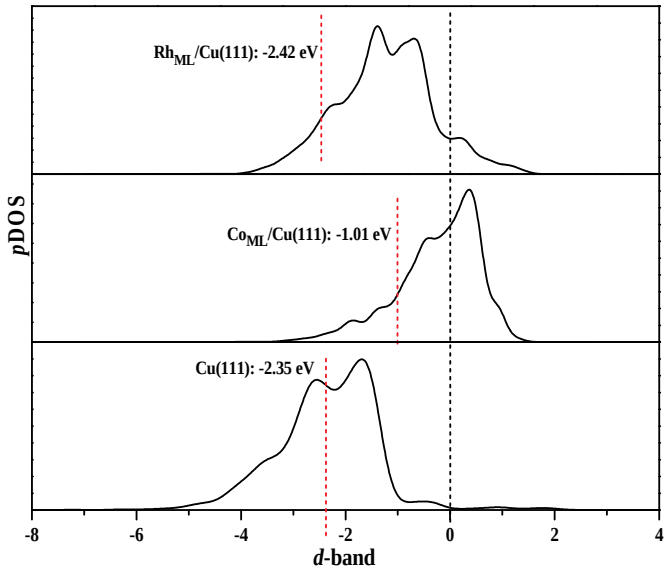

Fig. 8. The potential energy profile for *d*-band center of Rh_{ML}/Cu(111), Co_{ML}/Cu(111) and Cu(111) surfaces and the vertical dash lines indicate Fermi energy level.

selectivity, however, Co_{ML}/Cu(111) exhibits higher catalytic activity than Rh_{ML}/Cu(111), namely, the promoter Co monolayer presents higher catalytic activity than the promoter Rh monolayer, which is also supported by the previous studies [18] that CHO insertion over Co (0001) is more easier than that over Rh(111). Further, the *d*-band closer to Fermi level was favorable for CO insertion into CH_x by reducing the repulsion between CO and CH_x [58]. Similar mechanism can be applied to CHO insertion, namely, the shorter distance between the *d*-band center and Fermi level leads to the weak repulsion between CHO and CH_x, so Co_{ML}/Cu(111) exhibit higher catalytic activity towards CHO insertion than Rh_{ML}/Cu(111).

On the whole, the Rh monolayer-modified Cu(111) cannot improve the yield of C_2 oxygenates since methanol formation competes with CH_x formation. However, the Co monolayer-modified Cu(111) not only promotes the production of key CH_x intermediate and CHO insertion into CH_x to C_2 oxygenates to a great extent, but also inhibits methanol formation, which exhibits higher selectivity towards syngas conversion to form C_2 oxygenates. In addition, since Co_{ML}/Cu(111) is favorable for the formation of CH_2CHO, starting from CH_2CHO intermediate, the reactions related to CH_2CHO are examined (see Fig. S3), suggesting that CH_2CHO prefers to be hydrogenated to CH_3CHO in kinetics instead of its dissociation to CH + O and its hydrogenation to CH_2CHOH. Then, starting from CH_3CHO intermediate, it still prefers to be hydrogenated to CH_3CH_2O, followed by its hydrogenation to form ethanol. Namely, beginning with CH_2CHO intermediate, in the subsequent reactions, the dominant product is ethanol rather than the hydrocarbons, indicating that Co_{ML}/Cu(111) surface exhibits better selectivity towards ethanol formation, and the promoter Co is in favor of C—C chain formation leading to ethanol, however, it does not favored the further carbon chain growth due to the absence of C_2H_x intermediate.

4. Conclusion

In this study, aiming at identifying the effect of monolayer promoter Rh and Co on the selectivity of C_2 oxygenates over the promoter Rh and Co monolayer-modified Cu(111) in syngas conversion, the mechanism of syngas conversion to C_2 oxygenates on the promoter Rh and Co monolayer-modified Cu(111) surfaces, including the key intermediate CH_x formation and the C—C bond formation of C_2 oxygenates, has been examined using density functional theory calculations. The results show that CO initial activation via H-assisted mechanism is dominant to form CHO or COH, and all CH_x intermediate is produced via the C—O bond cleavage of CH_xO(x = 1–3) or CH_xOH(x = 1,2) species on the promoter Rh and Co monolayer-modified Cu(111). On the Rh monolayer-modified Cu(111), CH_xOH(x = 1,2) dissociation contributes to the favored CH_x(x = 1,2) monomers, which is competitive with CH_3OH formation. Whereas CH_2 is the favored monomer on the Co monolayer-modified Cu (111) surface, CH_2 formation is more favorable than CH_3OH formation. Compared to the single Cu(111) surface, the promoter Rh and Co monolayer-modified Cu(111) surfaces not only change the route of CH_x formation, but also alter the existence form of the favored CH_x monomer. More importantly, Co monolayer-modified Cu(111) inhibits methanol formation compared to the Cu(111), Rh(111), Co(111) and Rh_{ML}/Cu(111). As a result, the promoter Co monolayer-modified Cu (111) provides enough CH_x source to participate into the formation of C_2 oxygenates. Beginning with the favored CH_x monomers, the formation of C_2 oxygenates via CHO insertion into CH_x over the promoter Rh and Co monolayer-modified Cu(111) surface is the most favorable, moreover, the monolayer promoter Co presents better catalytic activity towards C_2 oxygenates formation than the monolayer promoter Rh.

Taking the formation of CH_x intermediate and the C—C bond formation of C_2 oxygenates into account, it is concluded that the promoter Co monolayer-modified Cu catalyst exhibits better selectivity towards the formation of C_2 oxygenates from syngas. On the other hand, electronic structure analysis revealed that the *d*-band center of the promoter Co monolayer-modified Cu(111) is the closest to Fermi level than the promoter Rh monolayer-modified Cu(111) and the single Cu(111), which results in the adsorption enhancement of CH_xO(x = 1–3) and CH_xOH(x = 1,2), promotes the C—O bond activation, and reduces the repulsion between CH_x and CHO. Hence, the monolayer promoter Co is beneficial to the formation of CH_x intermediate and C_2 oxygenates, which is very suitable for syngas conversion to C_2 oxygenates; this study provides a method for the design of high-performance catalyst with the monolayer metal-supported on other metal substrate in syngas conversion to C_2 oxygenates.

Acknowledgments

This work is financially supported by the Key projects of National Natural Science Foundation of China (No. 21736007), the National Natural Science Foundation of China (No. 21776193, 21476155), and the Top Young Innovative Talents of Shanxi.

Appendix A. Supplementary data

The detailed descriptions about the calculations methods of Gibbs free energy, the most stable configurations and key parameters of all adsorbed species on the promoter Rh and Co monolayer-modified Cu (111) surfaces, and the reactions related to CH_2CHO and CH_3CHO intermediates on Co_{ML}Cu(111) surface are presented. Supplementary data to this article can be found online at https://doi.org/10.1016/j.apsusc.2019.05.033.

References

[1] X.D. Xu, E.B.M. Doesburg, J.J.F. Scholten, Synthesis of higher alcohols from syngas-recently patented catalysts and tentative ideas on the mechanism, Catal. Today 2 (1987) 125–170.
[2] J.J. Spivey, A. Egbebi, Heterogeneous catalytic synthesis of ethanol from biomass-derived syngas, Chem. Soc. Rev. 36 (2007) 1514–1528.
[3] A.E. Farrell, Ethanol can contribute to energy and environmental goals, Science 311 (2006) 506–508.
[4] J. Goldemberg, Ethanol for a sustainable energy future, Science 315 (2007) 808–810.
[5] Y. Chen, H.T. Zhang, H.F. Ma, W.X. Qian, F.Y. Jin, W.Y. Ying, Direct conversion of syngas to ethanol over Rh–Fe/γ-Al_2O_3 catalyst: promotion effect of Li, Catal. Lett. 148 (2018) 691–698.
[6] R.G. Herman, Advances in catalytic synthesis and utilization of higher alcohols, Catal. Today 55 (2000) 233–245.
[7] M. Gupta, M.L. Smith, J.J. Spivey, Heterogeneous catalytic conversion of dry syngas to ethanol and higher alcohols on Cu-based catalysts, ACS Catal. 1 (2011) 641–656.
[8] J.L. Gong, H.R. Yue, Y.J. Zhao, S. Zhao, L. Zhao, J. Lv, S.P. Wang, X.B. Ma, Synthesis of ethanol via syngas on Cu/SiO_2 catalysts with balanced Cu^0-Cu^+ sites, J. Am. Chem. Soc. 134 (2012) 13922–13925.
[9] J. Yoshihara, S.C. Parker, A. Schafer, C.T. Campbell, Methanol synthesis and reverse water-gas shift kinetics over clean polycrystalline copper, Catal. Lett. 31 (1995) 313–324.
[10] L.C. Grabow, M. Mavrikakis, Mechanism of methanol synthesis on Cu through CO_2 and CO hydrogenation, ACS Catal. 1 (2011) 365–384.
[11] L.P. Han, D.S. Mao, J. Yu, Q.S. Guo, G.Z. Lu, Synthesis of C_2-oxygenates from syngas over Rh-based catalyst supported on SiO_2, TiO_2 and SiO_2–TiO_2 mixed oxide, Catal. Commun. 23 (2012) 20–24.
[12] N. Kapur, J. Hyun, B. Shan, J.B. Nicholas, K. Cho, Ab initio study of CO hydrogenation to oxygenates on reduced Rh terraces and stepped surfaces, J. Phys. Chem. C 114 (2010) 10171–10182.
[13] S.S.C. Chuang, R.W. Stevens Jr., R. Khatri, Mechanism of C_{2+} oxygenate synthesis on Rh catalysts, Top. Catal. 32 (2005) 225–232.
[14] D.H. Mei, R. Rousseau, S.M. Kathmann, V.A. Glezakou, M.H. Engelhard, W.L. Jiang, C.M. Wang, M.A. Gerber, J.F. White, D.J. Stevens, Ethanol synthesis from syngas over Rh-based/SiO_2 catalysts: a combined experimental and theoretical modeling study, J. Catal. 271 (2010) 325–342.
[15] Z. An, X. Ning, J. He, Ga-promoted CO insertion and C–C coupling on Co catalysts for the synthesis of ethanol and higher alcohols from syngas, J. Catal. 356 (2017) 157–164.
[16] R.G. Zhang, F. Liu, B.J. Wang, Co-decorated Cu alloy catalyst for C_2 oxygenate and ethanol formation from syngas on Cu-based catalyst: insight into the role of Co and Cu as well as the improved selectivity, Catal. Sci. Technol. 6 (2016) 8036–8054.
[17] L.X. Ling, Q. Wang, R.G. Zhang, D.B. Li, B.J. Wang, Formation of C_2 oxygenates and ethanol from syngas on an Fe-decorated Cu-based catalyst: insight into the role of Fe as a promoter, Phys. Chem. Chem. Phys. 19 (2017) 30883–30894.
[18] Y.H. Zhao, K.J. Sun, X.F. Ma, J.X. Liu, D.P. Sun, H.Y. Su, W.X. Li, Carbon chain growth by formyl insertion on rhodium and cobalt catalysts in syngas conversion, Angew. Chem. Int. Ed. 50 (2011) 5335–5338.
[19] G.R. Wang, R.G. Zhang, B.J. Wang, Insight into the preference mechanism for C-C chain formation of C_2 oxygenates and the effect of promoters in syngas conversion over Cu-based catalysts, Appl. Catal. A Gen. 466 (2013) 77–89.
[20] R.G. Zhang, G.R. Wang, B.J. Wang, L.X. Ling, Insight into the effect of promoter Mn on ethanol formation from syngas on a Mn-promoted MnCu(211) surface: a comparison with a Cu(211) surface, J. Phys. Chem. C 118 (2014) 5243−5254.
[21] W. Wang, Y. Wang, G.C. Wang, Ethanol synthesis from syngas over Cu(Pd)-doped Fe(100): a systematic theoretical investigation, Phys. Chem. Chem. Phys. 20 (2018) 2492–2507.
[22] X.C. Sun, R.G. Zhang, B.J. Wang, Insights into the preference of CH_x(x=1–3) formation from CO hydrogenation on Cu(111) surface, Appl. Surf. Sci. 265 (2013) 720–730.
[23] R.G. Zhang, G.R. Wang, B.J. Wang, Insights into the mechanism of ethanol formation from syngas on Cu and an expanded prediction of improved Cu-based catalyst, J. Catal. 305 (2013) 238–255.
[24] A.K. Dalai, B.H. Davis, Fischer–Tropsch synthesis: a review of water effects on the performances of unsupported and supported Co catalysts, Appl. Catal. A Gen. 348 (2008) 1–15.
[25] A.Y. Khodakov, W. Chu, P. Fongarland, Advances in the development of novel cobalt Fischer–Tropsch catalysts for synthesis of long-chain hydrocarbons and clean fuels, Chem. Rev. 107 (2007) 1692−1744.
[26] C.B. Chen, Q. Wang, G.R. Wang, B. Hou, L.T. Jia, D.B. Li, Mechanistic insight into the C_2 hydrocarbons formation from syngas on fcc-Co(111) surface: a DFT study, J. Phys. Chem. C 120 (2016) 9132−9147.
[27] R.G. Zhang, F. Liu, Q. Wang, B.J. Wang, D.B. Li, Insight into CH_x formation in Fischer–Tropsch synthesis on the hexahedron Co catalyst: effect of surface structure on the preferential mechanism and existence form, Appl. Catal. A Gen. 525 (2016) 76–84.
[28] Y.M. Choi, P. Liu, Mechanism of ethanol synthesis from syngas on Rh(111), J. Am. Chem. Soc. 131 (2009) 13054–13061.
[29] A. Deluzarche, J.P. Hindermann, R. Kieffer, R. Breault, A. Kiennemann, Ethanol formation mechanism from CO + H_2 on a Rh/TiO_2 catalyst, J. Phys. Chem. 88 (1984) 4993–4995.
[30] G. Prieto, S. Beijer, M.L. Smith, M. He, Y. Au, Z. Wang, D.A. Bruce, K.P. de Jong, J.J. Spivey, P.E. de Jongh, Design and synthesis of copper–cobalt catalysts for the selective conversion of synthesis gas to ethanol and higher alcohols, Angew. Chem. Int. Ed. 53 (2014) 6397–6401.
[31] K. Xiao, X.Z. Qi, Z.H. Bao, X.X. Wang, L.S. Zhong, K.G. Fang, M.G. Lin, Y.H. Sun, CuFe, CuCo and CuNi nanoparticles as catalysts for higher alcohol synthesis from syngas: a comparative study, Catal. Sci. Technol. 3 (2013) 1591–1602.
[32] B.H. Ren, X.Q. Dong, Y.Z. Yu, G.B. Wen, M.H. Zhang, A density functional theory study on the carbon chain growth of ethanol formation on Cu-Co(111) and (211) surfaces, Appl. Surf. Sci. 412 (2017) 374–384.
[33] X.C. Xu, J.J. Su, P.F. T, D.L. Fu, W.W. Dai, W. Mao, W.K. Yuan, J. Xu, Y.F. Han, First-principles study of C_2 oxygenates synthesis directly from syngas over CoCu bimetallic catalysts, J. Phys. Chem. C 119 (2015) 216−227.
[34] Q.L. Yang, A. Cao, N. Kang, H.Y. Ning, J.M. Wang, Z.T. Liu, Y. Liu, Bimetallic nano Cu−Co based catalyst for direct ethanol synthesis from syngas and its structure variation with reaction time in slurry reactor, Ind. Eng. Chem. Res. 56 (2017) 2889−2898.
[35] N.D. Subramanian, G. Balaji, C.S.S.R. Kumar, J.J. Spivey, Development of cobalt–copper nanoparticles as catalysts for higher alcohol synthesis from syngas, Catal. Today 147 (2009) 100–106.
[36] S. González, C. Sousa, F. Illas, Similarities and differences on the molecular mechanism of CO oxidation on Rh(111) and bimetallic RhCu(111) surfaces, Phys. Chem. Chem. Phys. 9 (2007) 2877–2885.
[37] R. Krishnamurthy, S.S.C. Chuang, K. Ghosal, Carbon monoxide adsorption and hydrogenation on Cu-Rh/SiO_2 catalysts, Appl. Catal. A Gen. 114 (1994) 109–125.
[38] F. Solymosi, J. Cserényi, Enhanced formation of ethane in the conversion of methane over Cu-Rh/SiO_2, Catal. Lett. 34 (1995) 343–350.
[39] Y.H. Zhao, M.M. Yang, D.P. Sun, H.Y. Su, K.J. Sun, X.F. Ma, X.H. Bao, W.X. Li, Rh-decorated Cu alloy catalyst for improved C_2 oxygenate formation from syngas, J. Phys. Chem. C 115 (2011) 18247–18256.
[40] J.J. Wang, P.A. Chernavskii, A.Y. Khodakov, Y. Wang, Structure and catalytic performance of alumina-supported copper–cobalt catalysts for carbon monoxide hydrogenation, J. Catal. 286 (2012) 51–61.
[41] S. Carenco, A. Tuxen, M. Chintapalli, E. Pach, C. Escudero, T.D. Ewers, P. Jiang, F. Borondics, G. Thornton, A.P. Alivisatos, H. Bluhm, J.H. Guo, M. Salmeron, Dealloying of cobalt from CuCo nanoparticles under syngas exposure, J. Phys. Chem. C 117 (2013) 6259−6266.
[42] J.R. Kitchin, J.K. Nørskov, M.A. Barteau, J.G. Chen, Role of strain and ligand effects in the modification of the electronic and chemical properties of bimetallic surfaces, Phys. Rev. Lett. 93 (2004) (156801-1–4).
[43] M.H. Shao, K. Shoemaker, A. Peles, K. Kaneko, L. Protsailo, Pt monolayer on porous Pd-Cu alloys as oxygen reduction electrocatalysts, J. Am. Chem. Soc. 132 (2010) 9253–9255.
[44] F.Y. Li, D.E. Jiang, X.C. Zeng, Z.F. Chen, Mn monolayer modified Rh for syngas-to-ethanol conversion: a first-principles study, Nanoscale 4 (2012) 1123–1129.
[45] P.L. Hansen, J.B. Wagner, S. Helveg, J.R. Rostrup-Nielsen, B.S. Clausen, H. Topsøe, Atom-resolved imaging of dynamic shape changes in supported copper nanocrystals, Science 295 (2002) 2053–2055.
[46] G. Kresse, J. Furthmüller, Efficient iterative schemes for ab initio total-energy calculations using a plane-wave basis set, Phys. Rev. B 54 (1996) 11169–11186.
[47] G. Kresse, J. Furthmüller, Efficiency of ab-initio total energy calculations for metals and semiconductors using a plane-wave basis set, Comput. Mater. Sci. 6 (1996) 15–50.
[48] J.P. Perdew, K. Burke, M. Ernzerhof, Generalized gradient approximation made simple, Phys. Rev. Lett. 77 (1996) 3865–3868.
[49] H.J. Monkhorst, J.D. Pack, Special points for Brillonin-zone integrations, Phys. Rev. B 13 (1976) 5188–5192.
[50] G. Henkelman, H. Jónsson, Improved tangent estimate in the nudged elastic band method for finding minimum energy paths and saddle points, J. Chem. Phys. 113 (2000) 9978–9985.
[51] R.A. Olsen, G.J. Kroes, G. Henkelman, A. Arnaldsson, H. Jónsson, Comparison of methods for finding saddle points without knowledge of the final states, J. Chem. Phys. 121 (2004) 9776–9792.
[52] G. Henkelman, B.P. Uberuaga, H. Jónsson, A climbing image nudged elastic band method for finding saddle points and minimum energy paths, J. Chem. Phys. 113 (2000) 9901–9904.
[53] X.M. Cao, R. Burch, C. Hardacre, P. Hu, An understanding of chemoselective hydrogenation on crotonaldehyde over Pt(111) in the free energy landscape: the microkinetics study based on first-principles calculations, Catal. Today 165 (2011) 71–79.
[54] R.G. Zhang, X.C. Sun, B.J. Wang, Insight into the preference mechanism of CH_x(x=1−3) and C−C chain formation involved in C_2 oxygenate formation from syngas on the Cu(110) surface, J. Phys. Chem. C 117 (2013) 6594−6606.
[55] H.Y. Zheng, R.G. Zhang, Z. Li, B.J. Wang, Insight into the mechanism and possibility of ethanol formation from syngas on Cu(100) surface, J. Mol. Catal. A Chem. 404–405 (2015) 115–130.
[56] X.C. Sun, Study on the Reaction Mechanism of Ethanol Synthesis from on cu Catalyst, Ms. D. Thesis Taiyuan University of Technology, 2013 June.
[57] B.Y. Han, X. Feng, L.X. Ling, M.H. Fan, Ping Liu, R.G. Zhang, B.J. Wang, CO oxidative coupling to dimethyl oxalate over Pd–Me(Me=Cu, Al) catalysts: a combined DFT and kinetic study, Phys. Chem. Chem. Phys. 20 (2018) 7317−7332.
[58] R.G. Zhang, G.X. Wen, H. Adidharma, A.G. Russell, B.J. Wang, M. Radosz, M.H. Fan, C_2 oxygenate synthesis via Fischer−Tropsch synthesis on Co_2C and Co/Co_2C interface catalysts: how to control the catalyst crystal facet for optimal selectivity, ACS Catal. 7 (2017) 8285−8295.